

## Robustness Issues in Intelligent Structures Using Nonconvex and Nonsmooth Optimization

Amalia Moutsopoulou<sup>1\*</sup>, Georgios Stavroulakis<sup>2</sup>, Tasos Pouliezos<sup>2</sup>

<sup>1</sup>Department of Mechanical Engineering, Hellenic Mediterranean University, Estavromenos, Heraklion Crete, Greece

<sup>2</sup>Department of Production Engineering and Management, Technical University of Crete, Kounoupidianna GR-73100 Chania, Greece

\*Corresponding Author: Amalia Moutsopoulou, Department of Mechanical Engineering, Hellenic Mediterranean University, Estavromenos, Heraklion Crete, Greece

### ABSTRACT

An accurate model of a homogeneous intelligent structure is derived by means of the finite element analysis. A robust controller is designed based on the augmented plant composed of the nominal model and its accompanied uncertainty by solving a convex optimization problem. The robustness of the uncertain closed-loop model and the effect of performance index weights on the system output are investigated. An optimal controller is using nonconvex and nonsmooth optimization to mimic the previous controller.

**Keywords:** Smart structures, robust control, finite elements formulation, optimization.

### INTRODUCTION

This paper describes an integrated approach to design and implement robust controllers for intelligent structures. An intelligent structure is the structure that monitors itself and its environment. In our paper we use a smart piezoelectric structure [1], [2]. An accurate model of a homogeneous beam with piezoelectric actuators and sensors is derived by means of the finite element analysis. A robust controller with is designed based on the augmented plant composed of the nominal model and its accompanied uncertainty by solving a convex optimization problem. The mathematical model derived using robust control is compared with models obtained by more conventional and well-known methods [3], [4]. Using this model, an  $H_{\infty}$  controller is designed for vibration suppression purposes. An optimal controller is designed using nonconvex and nonsmooth optimization [5], [6]. Robust control theory is used to synthesize controllers achieving stabilization with guaranteed performance for smart structures. To use  $H_{\infty}$  methods, a control designer expresses the control problem as a mathematical optimization problem and then finds the controller that solves this optimization [7], [8]. This article shows some steps that should be followed in the design of a smart structure. In our paper a cantilever slender beam with rectangular cross-sections is considered. Thirty-six pairs of piezoelectric patches are embedded

symmetrically at the top and the bottom surfaces of the beam, as a model structure. It is obvious that every structure modelled by using finite elements can be used in a similar way. The beam is from graphite- epoxy T300 – 976 and the piezoelectric patches are PZT G1195N. The top patches act like sensors and the bottom like actuators [9], [10]. The resulting composite beam is modelled by means of the classical laminated technical theory of bending. Let us assume that the mechanical properties of both the piezoelectric material and the host beam are independent in time. The thermal effects are considered to be negligible as well [5], [7], [11].

**Table1.** Parameters of The Composite Beam

Parameters	Values
Beam length, L	0.8m
Beam width, W	0.08m
Beam thickness, h	0.0093m
Beam density, $\rho$	1800kg/m <sup>3</sup>
Young's modulus of the beam, E	$1.5 \times 10^{11}$ N/m <sup>2</sup>
Piezoelectric constant, d <sub>31</sub>	$254 \times 10^{-12}$ m/V
Electric constant, $\xi_{33}$	$11.5 \times 10^{-3}$ V m/N
Young's modulus of the piezoelectric element	$1.5 \times 10^{11}$ N/m <sup>2</sup>
Width of the piezoelectric element	$b_s = b_a = 0.07$ m
Thickness of the piezoelectric element	$h_s = h_a = 0.0002$ m

The beam has length L, width W and thickness h. The sensors and the actuators have width  $b_s$  and

bA and thickness hS and hA, respectively. The electromechanical parameters of the beam of interest are given in the Table I, [12], [13]

In order to derive the basic equations for piezoelectric sensors and actuators [14], [15], [16], [17], [18].

we assume that:

- The piezoelectric sensors actuators (S/A) are bonded perfectly on the host beam;
- The piezoelectric layers are much thinner than the host beam;
- The piezoelectric material is homogeneous, transversely isotropic and linearly elastic;

### RESEARCH ON INTELLIGENT STRUCTURES

The following paragraphs give the research work done on the intelligent structures so far. Culshaw discussed the concept of smart structure, its benefits and applications [8]. Rao and Sunar explained the use of piezo materials as sensors and actuators in sensing vibrations in their survey paper [19]. Hubbard and Baily have studied the application of piezoelectric materials as sensor / actuator for flexible structures [14]. Hanagud developed a Finite Element Model (FEM) for a beam with many distributed piezoceramic sensors / actuators [20].

Packard presented a new finite element (FE) modeling technique for flexible beams [21]. Continuous time and discrete time algorithms were proposed to control a thin piezoelectric structure by Bona [22]. Schiehlen and Schonerstedt reported the optimal control designs for the first few vibration modes of a cantilever beam using piezoelectric sensors / actuators [18]. Choi have shown a design of position tracking sliding mode control for a smart structure [7]. Distributed controllers for flexible structures can be seen in Forouza Pourki [10].

A FEM approach was used by Benjeddou to model a sandwich beam with shear and extension piezoelectric elements [1]. The finite element model employed the displacement field of Zhang and Sun [23]. It was shown that the finite element results agree quite well with the analytical results. Raja extended the finite element model of Benjeddou's research team to include a vibration control scheme [1], [24]. A recent review of single and multilayer models suitable for smart structures has been published by Tairidis [25].

### THEORETICAL FORMULATION

The dynamical description of the system is given in the finite element discretized structure

framework by,

$$M\ddot{q}(t) + D\dot{q}(t) + Kq(t) = f_m(t) + f_e(t) \tag{1}$$

where M is the generalized mass matrix, D the viscous damping matrix, K the generalised stiffness matrix,  $f_m$  the external loading vector and  $f_e$  the generalised control force vector produced by electromechanical coupling effects. The independent variable  $q(t)$  is composed of transversal deflections  $w_i$  and rotations  $\psi_i$ , i.e. [12], [13], [26].

Furthermore to express  $f_e(t)$  as  $B_u(t)$  we write it as  $f_e^* u$ , where  $f_e^*$  is the piezoelectric force for a unit applied on the corresponding actuator, and u represents the voltages on the actuators. Lastly  $d(t)=f_m(t)$  is the disturbance vector.

### CONTROL DESIGN

We solve a regulator problem for the smart beam with viscous layer. The objective in this section is to determine the optimal vector of active control forces  $u(t)$  subjected to performance criteria and satisfying the dynamical equations of the system, such that to reduce in an optimal way the external excitations. We consider the steady state (infinite time) case, i.e. the optimization horizon is allowed to extend to infinity. We seek a linear state feedback [20], [27], [28].

$$u(t) = -K x(t), \text{ with constant gain } K.$$

The control problem is to keep the beam in equilibrium which means zero displacements and rotations in the face of external disturbances, noise and model inaccuracies, using the available measurements (displacement) and controls [13], [21], [29].

### H INFINITY CONTROL

To relate the structures used in classical and  $H_{\infty}$  control, let's look at Fig. 1 Control bloc diagram, in the frequency domain [30], [31], [32].

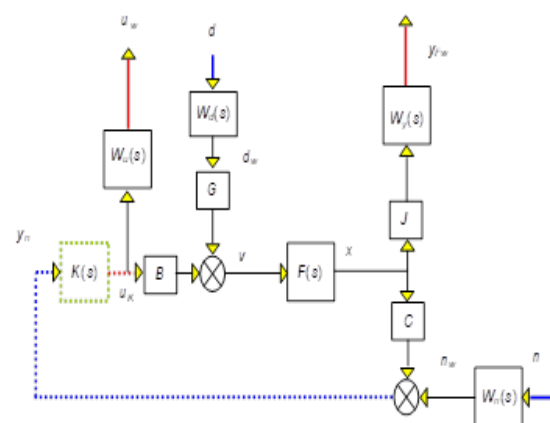


Fig1. Control bloc diagram in the frequency domain1.

In this diagram are included all inputs and outputs of interest, along with their respective weights  $W$ , where  $W_d$ ,  $W_u$ ,  $W_n$ ,  $W_y$  are the weights for the disturbances, control, noise, outputs respectively. The exogenous inputs are the noise  $n$  and the disturbances  $d$ .  $K(s)$  is the controller,  $B$ ,  $G$ ,  $x$ ,  $y$ ,  $C$  define the state form of the system,  $x$  is the input  $y$  is the output and  $F(s)$  is the transfer function of our system [16], [20], [33].

To find the necessary transfer functions, one first considers the description of the controlled system:

$$yFw = W_y Jx = W_y JFv = W_y JF(GW_d d + Bu_K) = W_y JFGW_d d + W_y JFBu_K$$

$$u_w = W_u u_K \tag{2}$$

$$y_n = Cx + W_n n = CFv + W_n n$$

$$= CF(GW_d d + Bu_K) + W_n n$$

$$= CFGW_d d + CFBu_K + W_n n$$

Combining all these gives,

$$\begin{bmatrix} u_w \\ y_{Fw} \\ y_n \end{bmatrix} = \begin{bmatrix} 0 & 0 & \dots & W_u \\ W_y JFGW_d & 0 & \dots & W_y JFB \\ \dots & \dots & W_n & \dots \\ CFGW_d & W_n & \dots & CFB \end{bmatrix} \begin{bmatrix} d \\ n \\ u_K \end{bmatrix} \tag{3}$$

Note that the plant transfer function matrix,  $F(s)$ , is reduced from the suitably reformulated plant equations,

$$\dot{x}(t) = Ax(t) + Iv(t)$$

$$y(t) = Ix(t)$$

where  $v(t) = Gd + Bu_K$ . Hence,

$$F(s) = (sI - A)^{-1} \tag{4}$$

The equivalent two-port diagram in the state space form is Fig. 2 for the close loop, and with more details in Fig. 3 [16], [30],

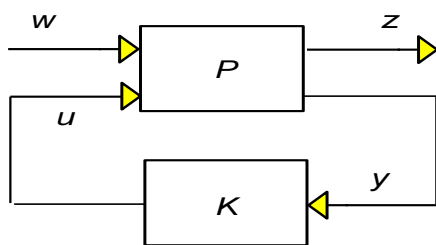


Fig2. Two-port diagram.

with,

$$z = \begin{bmatrix} u_w \\ y_{Fw} \end{bmatrix}, \quad w = \begin{bmatrix} d \\ n \end{bmatrix}, \quad y = y_n, \quad u = u_K \tag{5}$$

where  $z$  are the output variables to be controlled,

and  $w$  the exogenous inputs [17], [26], [29]

Given that  $P$  has two inputs and two outputs it is, as usual, naturally partitioned as,

$$\begin{bmatrix} z(s) \\ y(s) \end{bmatrix} = \begin{bmatrix} P_{zw}(s) & P_{zu}(s) \\ P_{yw}(s) & P_{yu}(s) \end{bmatrix} \begin{bmatrix} w(s) \\ u(s) \end{bmatrix} \stackrel{op}{=} P(s) \begin{bmatrix} w(s) \\ u(s) \end{bmatrix} \tag{6}$$

Also,

$$u(s) = K(s)y(s). \tag{7}$$

Using (3) the transfer function for  $P$  is

$$P(s) = \begin{bmatrix} 0 & 0 & \dots & W_u \\ W_y JFGW_d & 0 & \dots & W_y JFB \\ \dots & \dots & W_n & \dots \\ CFGW_d & W_n & \dots & CFB \end{bmatrix} \tag{8}$$

while the closed loop transfer function  $M_{zw}(s)$  is,

$$M_{zw}(s) = P_{zw}(s) + P_{zu}(s)K(s)(I - P_{yu}(s)K(s))^{-1}P_{yw}(s) \tag{9}$$

or,

$$z = M_{zw} w = F_l(P, K) w \tag{10}$$

Equation (9) is the well-known lower LFT for  $M_{zw}$ .

To express  $P$  in state space form, the natural partitioning,

$$P(s) = \left[ \begin{array}{c|cc} A & B_1 & B_2 \\ \hline C_1 & D_{11} & D_{12} \\ C_2 & D_{21} & D_{22} \end{array} \right] = \begin{bmatrix} P_{zw}(s) & P_{zu}(s) \\ P_{yw}(s) & P_{yu}(s) \end{bmatrix} \tag{11}$$

is used (where the packed form has been used), while the corresponding form for the controller  $K$  is [9], [10], [33],

$$K(s) = \left[ \begin{array}{c|c} A_K & B_K \\ \hline C_K & D_K \end{array} \right]$$

Equation (11) defines the equations at the state space form,

$$\dot{x}(t) = Ax(t) + [B_1 \ B_2] \begin{bmatrix} w(t) \\ u(t) \end{bmatrix}$$

$$\begin{bmatrix} z(t) \\ y(t) \end{bmatrix} = \begin{bmatrix} C_1 \\ C_2 \end{bmatrix} x(t) + \begin{bmatrix} D_{11} & D_{12} \\ D_{21} & D_{22} \end{bmatrix} \begin{bmatrix} w(t) \\ u(t) \end{bmatrix}$$

and,

$$\dot{x}_K(t) = A_K x_K(t) + B_K y(t)$$

$$u(t) = C_K x_K(t) + D_K y(t)$$

To find the matrices involved, we break the feedback loop and use the relevant equations:

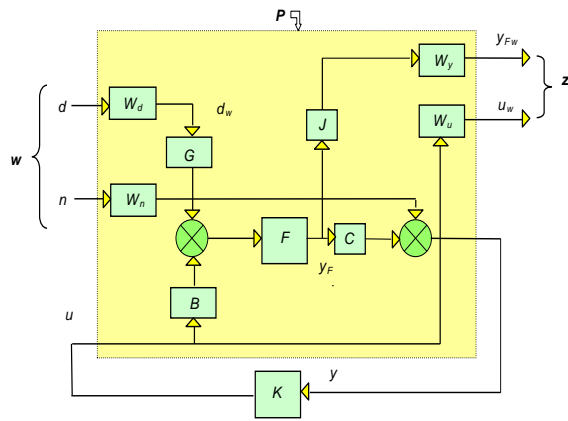


Fig3. Details of  $H_\infty$  structure

Therefore the equations relating the inputs, outputs, states and input/output to the controller are [31], [26]:

$$\begin{aligned} \dot{x}_F &= Ax_F + (Gd_w + Bu), & y_F &= x_F \\ \dot{x}_u &= A_u x_u + B_u u, & u_w &= C_u x_u + D_u u \\ \dot{x}_{y_F} &= A_{y_F} x_{y_F} + B_{y_F} J y_F, & y_{Fw} &= C_{y_F} x_{y_F} + D_{y_F} y_F \\ \dot{x}_n &= A_n x_n + B_n n, & n_w &= C_n x_n + D_n n \\ \dot{x}_d &= A_d x_d + Gd, & d_w &= C_d x_d + D_d d \\ y_n &= C y_F + n_w \end{aligned} \quad (12)$$

$$x = \begin{bmatrix} x_F \\ x_u \\ y_{Fw} \\ x_n \\ x_d \end{bmatrix}, \quad y = y_n, \quad w = \begin{bmatrix} d \\ n \end{bmatrix}, \quad z = \begin{bmatrix} u_w \\ y_{Fw} \end{bmatrix}, \quad u = u_K$$

From (12), we use  $d_w$ ,  $n_w$  and  $y_{Fw}$  and take our initial state space equation of our system [13], [26]

$$\dot{x} = \begin{bmatrix} A_G & 0 & 0 & 0 & GC_d \\ 0 & A_u & 0 & 0 & 0 \\ BC_F & 0 & A_{y_F} & 0 & 0 \\ 0 & 0 & 0 & A_n & 0 \\ 0 & 0 & 0 & 0 & A_d \end{bmatrix} x + \begin{bmatrix} GD_d & 0 \\ 0 & 0 \\ 0 & 0 \\ 0 & B_n \\ B_d & 0 \end{bmatrix} w + \begin{bmatrix} B \\ B_u \\ 0 \\ 0 \\ 0 \end{bmatrix} u \quad (13)$$

$$z = \begin{bmatrix} 0 & C_u & 0 & 0 & 0 \\ D_{y_F} C_F & 0 & C_{y_F} & 0 & 0 \end{bmatrix} x + 0w + \begin{bmatrix} D_u \\ 0 \end{bmatrix} u \quad (14)$$

$$y = [C_F \quad 0 \quad 0 \quad C_n \quad 0]x + [0 \quad D_n]w + 0u \quad (15)$$

Therefore the matrices are:

$$A_1 = \begin{bmatrix} A_F & 0 & 0 & 0 & GC_d \\ 0 & A_u & 0 & 0 & 0 \\ BC_F & 0 & A_{y_F} & 0 & 0 \\ 0 & 0 & 0 & A_n & 0 \\ 0 & 0 & 0 & 0 & A_d \end{bmatrix}, \quad B_1 = \begin{bmatrix} GD_d & 0 \\ 0 & 0 \\ 0 & 0 \\ 0 & B_n \\ B_d & 0 \end{bmatrix}, \quad B_2 = \begin{bmatrix} B \\ B_u \\ 0 \\ 0 \\ 0 \end{bmatrix}$$

$$C_1 = \begin{bmatrix} 0 & C_u & 0 & 0 & 0 \\ D_{y_F} C_F & 0 & C_{y_F} & 0 & 0 \end{bmatrix}, \quad D_{11} = 0, \quad D_{12} = \begin{bmatrix} D_u \\ 0 \end{bmatrix} \quad (16)$$

$$C_2 = [C_F \quad 0 \quad 0 \quad C_n \quad 0], \quad D_{21} = [0 \quad D_n], \quad D_{22} = 0$$

Robust control allows dealing with uncertainty affecting a dynamical system and its environment. In this section, we assume that we have a mathematical model of the dynamical system with uncertainty. We restrict ourselves to linear systems: if the dynamical system we want to control has some nonlinear components (e.g., input saturation), they must be embedded in the uncertainty model. Similarly, we assume that the control system is relatively small scale (low number of states): higher-order dynamics are embedded in the uncertainty model [11], [20], [27].

### NONCONVEX NONSMOOTH ROBUST OPTIMIZATION

The main difficulties faced when seeking a feedback matrix  $K(s)$  are as follows:

#### Nonconvexity

The stability conditions are typically nonconvex in  $K(s)$ ;

#### Non Differentiability

The performance criterion to be optimized is typically a nondifferentiable function of  $K(s)$ ;

#### Robustness

Stability and performance should be ensured for every possible instance of the uncertainty.

So if we are to formulate the robust control problem as an optimization problem, we should be ready to develop and use techniques from nonconvex, nondifferentiable, robust optimization [29], [32].

### INPUTS

A typical wind load Fig. 3 acting on the side of the structure. The wind load is a real life wind speed measurements in relevance with time that took place in Estavromenos of Heraklion Crete. We transform the wind speed in wind pressure function  $f_m(t)$  has been obtained from the wind velocity record, through the relation

$$f_m(t) = \frac{1}{2} \rho C_u V^2(t) \quad (17)$$

where  $V$ =velocity,  $\rho$ =density and  $C_u=1.5$ .



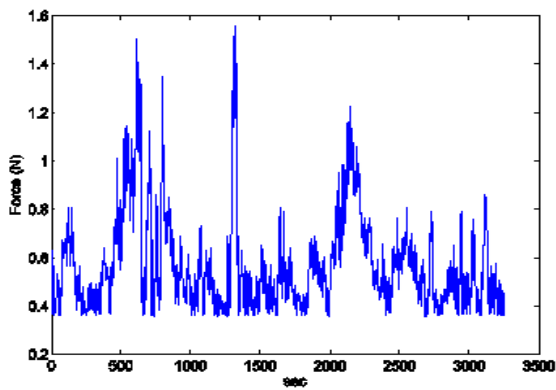


Fig4. Wind load

Moreover, in all simulations, random noise has been introduced to measurements at system output locations within a probability interval of  $\pm 1\%$ . Due to small displacements of system nodal points, noise amplitude is taken to be small, of the order of  $5 \times 10^{-5}$ . On the other hand, the signal is introduced at each node of the beam by a different percentage, that percentage being lower at the first node due to the fact that the beam end point is clamped [23], [26], [34].

RESULTS

Furthermore, we control the structure with variations of the nominal values of the mass matrix  $M$ , stiffness matrix  $K$ . In Figs. 4a-b complete vibration reduction is achieved even for variations of beam mass and stiffness up to 80%. The piezoelectric force is in their endurance limits, less 500 Volt 9 (Fig. 4c). In Figs. 5a-b complete vibration reduction is achieved even for variations of matrices  $A$  and  $B$  up to 90%. Moreover, controller size contains so as to lower energy consumption and maintain piezoelectric materials within operation limits (500 volt), Fig. 5c.

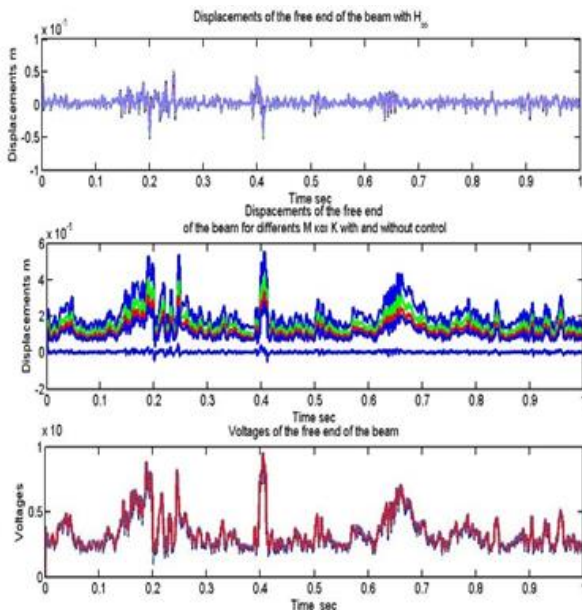


Fig4a. Displacement of the free end of the beam with

$H_{\infty}$  control.

Fig4b. Displacement of the free end of the beam for different prices of the Mass and the stiffness matrices with and without control.

Fig4c. Control voltages for the free end of the beam with  $H_{\infty}$  control.

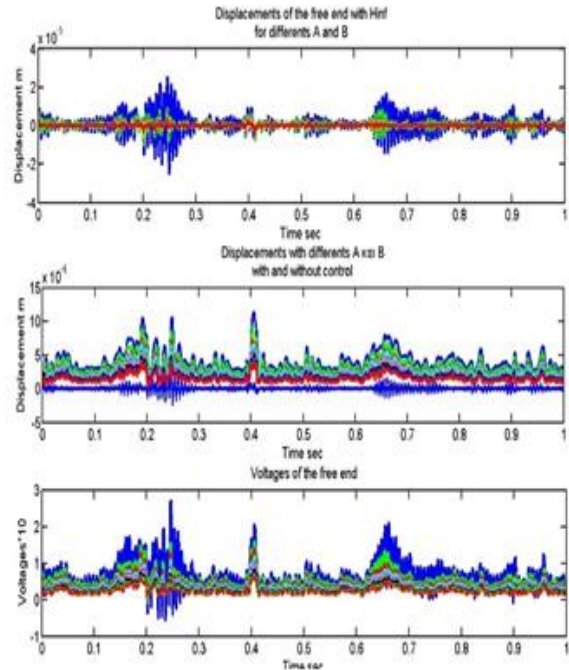


Fig5a. Displacement of the free end of the beam with  $H_{\infty}$  control

Fig5b. Displacement of the free end of the beam for different prices of the matrices A and B of the system with and without control

Fig5c. Control voltages for the free end of the beam with  $H_{\infty}$  control.

NONSMOOTH AND NONCONVEX OPTIMIZATION

The  $H_{\infty}$  controller found is of order 36. The fact that controller order, which is equal to the order of the system, is relatively higher than the order of classical controllers such as  $PI$  and  $LQR$  has led a number of researchers to develop order reduction algorithms. The most widely used such algorithm, known as HIFOO, has been implemented in a Matlab environment, and is the one used in the following procedure [3], [4], [5], [6].

The general problem is to compute a controller of reduced rank/order  $n < 36$  while retaining the performance of the  $H_{\infty}$  criterion as well as the behavior of a full order controller for the given system [2], [3], [4], [5].

$$\begin{aligned}
 \dot{x}(t) &= Ax(t) + B_1w(t) + B_2u(t) \\
 z(t) &= C_1x(t) + D_{11}w(t) + D_{12}u(t) \\
 y(t) &= C_2x(t) + D_{21}w(t) + D_{22}u(t)
 \end{aligned}
 \tag{18}$$

The state space equations for the controller K are

$$\begin{aligned} \dot{x}_K(t) &= A_{K \times K}(t) + B_K y(t) \\ u(t) &= C_{K \times K}(t) + D_K y(t) \end{aligned} \quad (19)$$

Let  $\alpha(X)$  be the spectral abscissa of a matrix X, that is the maximum real part of its eigenvalues. Then, we require not only that  $\alpha(ACL) < 0$ , where ACL is the closed-loop system matrix, but that  $\alpha(Ak) < 0$  as well. The feasible set of Ak, that is the set of stable matrices, is not a convex set and has a boundary that is not smooth [3], [4], [5], [16].

The HIFOO procedure has two phases: stability and performance optimization [3], [4], [6], [29], [32].

In the stability phase, HIFOO attempts to minimize

$$\max(\alpha(A_{CL}, \epsilon \alpha(A_{CL})) \quad (20)$$

where  $\epsilon$  is a positive parameter that will be described shortly, until a controller is found for which this quantity is negative, that is the controller is stable and makes the closed-loop system stable. In case it is unable to find such a controller, HIFOO terminates unsuccessfully.

In the performance optimization phase, HIFOO searches for a local minimizer of

$$f(K) = \begin{cases} \infty, & \text{if } \max(a(A_a), a(A_k)) \geq 0 \\ \max(\|T_{zw}\|_{\infty}, \epsilon \|K\|_{\infty}), & \text{else} \end{cases} \quad (21)$$

where

$$\|K\|_{\infty} = \sup_{R_s=0} \|C_k (sI - A_k)^{-1} B_k + D_k\|_2$$

The introduction of  $\epsilon$  is motivated by the fact that the main design objective is to attain closed-loop system stability and to minimize  $\|T_{zw}\|_{\infty}$ , by demonstrating that  $\epsilon$  should be relatively small; the term  $\epsilon \|K\|_{\infty}$ , however, prevents the controller  $H_{\infty}$  norm from becoming too large, in which case the stability constraint by itself would not exist. Given that it is preceded by the stability phase, the performance optimization phase is initialized with a finite value of  $f(K)$ . Consequently, when it reaches a value of K for which

$f(K)=\infty$ , that value is rejected, since an objective reduction is sought at each iteration [5], [16], [32].

As mentioned before, the HIFOO controller is implemented in Matlab by way of appropriate routines. It is called in the following manner:

$$K_{foo} = hifoo(\text{plant}, 2)$$

where plant is the system description in the form of Eq. (18), and n = 2 is controller order.

The resulting controller is described in state space in similar manner as  $H_{\infty}$ , i.e.

$$\begin{aligned} \dot{x}_K(t) &= A_{K \times K}(t) + B_K y(t) \\ u(t) &= C_{K \times K}(t) + D_K y(t) \end{aligned} \quad (22)$$

The controller state space equation is given by (22), where controller matrices are equal to

$$\begin{aligned} A_K &= \begin{bmatrix} 728.1 & -5034 \\ 207.5 & -1408 \end{bmatrix} \\ B_K &= \begin{bmatrix} 212.8 & 811.6 & 1716 & 2810 \\ -164.9 & -637.2 & -1348 & -2207 \end{bmatrix} \\ C_K &= \begin{bmatrix} 1557 & -916.7 \\ 1013 & -592.3 \\ 517 & -297.9 \\ 144.3 & -82.59 \end{bmatrix} \\ D_K &= \begin{bmatrix} 36.1 & 136.6 & 287.1 & 468.3 \\ 23.5 & 87.69 & 186.5 & 303 \\ 12.12 & 44.12 & 93.39 & 154.3 \\ 4.204 & 12.53 & 26.92 & 43.51 \end{bmatrix} \end{aligned} \quad (23)$$

For the purpose of comparison of HIFOO controller performance to that of  $H_{\infty}$ , the beam free end response is examined, for the mechanical input [29], [32].

For the input, in Fig. 6 the beam free end response is shown, initially with and then without the HIFOO controller, while Fig. 7 presents produced actuator voltage using the HIFOO controller.

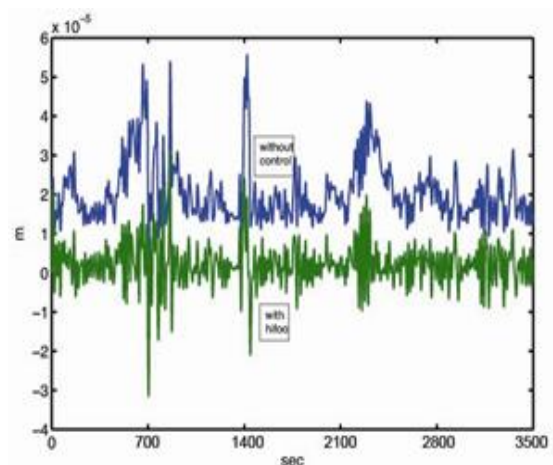


Fig6. Beam free end displacement, with and without HIFOO control

Using the HIFOO controller for an actual wind loading, beam position control is effected with node displacements of order of  $10^{-5}$ , with lower produced voltage. We therefore maintain  $H_{\infty}$

criterion performance with a lower order controller. The maximum produced voltage for the HIFOO controller is 7 V; the respective value is 45 V for the  $H_\infty$  controller. In other words, beam adjustment to its equilibrium position is achieved with a lower order controller that requires lower voltage, Fig.7

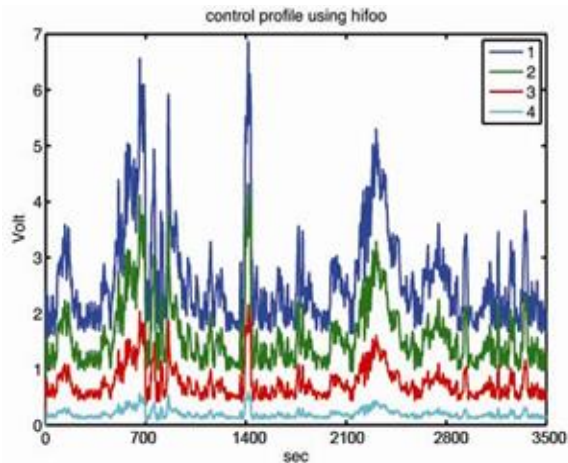


Fig7. Stress at beam nodal points, using HIFOO.

## CONCLUSIONS

This paper describes an integrated approach to design and implement robust controllers for smart structures. The mathematical model derived using robust control is compared with models obtained by more conventional and well-known methods. Using this model, a *Hinfinity* controller is designed for vibration suppression purposes. This robust controller accommodates the limited control effort produced by actuators. *Hinfinity* techniques have the advantage over classical control techniques in that they are readily applicable to problems involving multivariate systems with cross-coupling between channels. Simultaneously optimizing robust performance and robust stabilization is difficult. One method that comes close to achieving this is *Hinfinity*, which allows the control designer to apply classical loop-shaping concepts to the multivariable frequency response to get good robust performance, and then optimizes the response near the system bandwidth to achieve good robust stabilization. The Bode's integrals are used to approximate the derivatives of amplitude and phase of the plant model with respect to the frequency. Simulation examples illustrate the effectiveness and the simplicity of the proposed method to design the robust controllers. An optimal controller is the trained using nonconvex and nonsmooth optimization to mimic the previous controller. These designs are all then realized as digital controllers and their closed-loop performances have been compared. In particular, the robustness

properties of the controller have been verified for variations in the mass of the test article and the sampling time of the controller.

## REFERENCES

- [1] A. Benjeddou, M. A. Trindade, R. Ohayon, "New shear actuated smart structure beam finite element," *Journal of Guidance, Dynamics and Control*, vol. 37, pp. 378-383, 1999.
- [2] O. Bosgra, H. Kwakernaak "Design methods for control systems". Course notes, Dutch Institute for Systems and Control. 2001;67.
- [3] J. Burke, D. Henrion, A. Lewis, M.L. Overton ML. HIFOO a Matlab package for fixed-order controller design and  $H_1$  optimization. 2006.
- [4] J. V. Burke, D. Henron, A. S. Lewis, M. L. Overton, "Stabilization via Nonsmooth, Nonconvex Optimization," *Automatic Control IEE*, 2006, vol. 5, Issue 11, pp. 1760–1769.
- [5] J. Burke, A. Lewis, M.L. Overton "A robust gradient sampling algorithm for nonsmooth nonconvex optimization". *Siam Journal on Optimization*. Vol. 15, pp. 751-779, 2005.
- [6] J. Burke, M.L. Overton "Variational analysis of Non-Lipscitz spectral functions". *Mathematical Programming*. Vol. 90, pp. 317-352, 2001.
- [7] Seung-Bok Choi, Chae-Cheon Cheong, Chul-Hea Lee, "Position tracking control of a smart flexible structure featuring a piezofilm actuator." *Journal of Guidance and Control*. vol. 19, no. 6, pp. 1364-1369, 1996.
- [8] B. Culshaw. Smart structures, "A concept or a reality." *Journal of Systems and Control Engg.*, vol.26, no. 206, 1992.
- [9] J. C. Doyle, K. Glover, P. Khargoneker, B. Francis, "State space solutions to standard  $h_2$  and  $h_\infty$  control problems," *IEE Trans. Automatic Control*, vol. 34, pp. 831–847.
- [10] P. Forouza, "Distributed controllers for flexible structures using piezoelectric actuators/sensors." *Proc. 32nd IEEE CDC Conf.*, Texas, USA, pp. 1367-1369, December. 1993.
- [11] B. A. Francis, *A course on  $H_\infty$  control theory*, Springer - Verlag. 1987.
- [12] J. Friedman, K. Kosmatka, "An improved two node Timoshenko beam finite element," *J. Computer and Structures*, vol 47, pp. 473-481, 1993.
- [13] A. Moutsopoulou, A. Pouliezios, G. E. Stavroulakis, "Modelling with Uncertainty and Robust Control of Smart Beams," Paper 35, *Proceedings of the Ninth International Conference on Computational Structures Technology*. B.H.V. Topping and M. Papadrakakis, (Editors), Civil Comp Press, 2008.
- [14] T. Baily, J.E. Hubbard, "Distributed piezoelectric polymer active vibration control of a cantilever beam," *Journal of Guidance, Dynamics and Control*, vol.8, no. 5, pp. 605-611, 1985.



- [15] B. Bandyopadhyay, T. C. Manjunath, M. Unapathy, Modeling, Control, and Implementation of Smart Structures, Springer ISBN-10 3-540-48393-4, 2007.
- [16] D. Hinrichsen, A.J. Pritchard “Mathematical Systems Theory I: Modelling, State Space Analysis. Stability and Robustness”. Springer. 2005;134.
- [17] H.F. Tiersten, “Linear Piezoelectric Plate Vibrations”. Plenum Press. New York. Tits AL, Yang, Y. Globally convergent algorithms for robust pole assignment by state feedback. IEEE Trans. on Automatic Control. Vol. 41, pp. 1432-1452, 1996.
- [18] W. Schiehlen, H. Schonerstedt, “Controller design for the active vibration damping of beam structure,” Proc. Smart Mechanical Systems Adaptronics SAE International. USA. pp. 1137-146, 1998.
- [19] S. Rao, M. Sunar, “Piezoelectricity and its uses in disturbance sensing and control of flexible structures,” A survey. Applied mechanics Rev. vol. 17, no.2, pp. 113-119, 1994.
- [20] S. Hanagud, M.W. Obal, A. J. Callise, “Optimal vibration control by the use of piezoelectric sensors and actuators.” J. Contr. Guidance, vol. 15, no. 5, pp.1199-1206, 1992.
- [21] A. Packard, J. Doyle, G. Balas “Linear, multivariable robust control with a  $\mu$  perspective”. ASME Journal of Dynamic Systems, Measurement and Control, 50th Anniversary Issue. Vol. 115, no. 2b, pp. 310–319, 1993.
- [22] B. Bona, M. Indri, A. Tornamable, “Flexible piezoelectric structures approximate motion equations and control algorithms,” IEEE Auto. Contr., vol. AC-42, no. 1, pp.94-101, 1997.
- [23] X. D. Zhang, C. T. Sun, “Formulation of an adaptive sandwich beam,” Smart Materials and Structures Journal, vol. 5, no. 6, pp. 814-823, 1996.
- [24] S. Raja, G. Prathap, P. K, “Sinha Active vibration control of composite sandwich beams with piezoelectric extension-bending and shear actuators,” J. Smart Materials and Structures, vol. 11, no. 1, pp. 63-71, 2002.
- [25] G. Tairidis, G. Foutsitzi, G.E. Stavroulakis “A Multi-layer Piezocomposite Model and Application on Controlled Smart Structures”. In: H. Altenbach, F. Jablonski, W. Müller, K. Naumenko, P. Schneider (eds) Advances in Mechanics of Materials and Structural Analysis. Advanced Structured Materials. Springer, Cham. No 80, 2018.
- [26] G. E. Stavroulakis, G. Foutsitzi, E. Hadjigeorgiou, D. Marinova, C. C. Baniotopoulos, “Design and robust optimal control of smart beams with application on vibrations suppression,” Advances in Engineering Software. vol.36, Issues 11-12, pp. 806–813, 2005.
- [27] D. Halim Vibration Analysis and Control of Smart Structures, Doctor of Philosophy. 2002.
- [28] D. Halim, SOR. Moheiman “Spatial resonant control of °exible structures - application to a piezoelectric laminate beam”. Control Systems Technology. Vol. 9, no. 1, pp. 37-53, 2001.
- [29] S. M. Yang and Y. J. Lee, “Optimization of non-collocated sensor, actuator location and feedback gain and control systems,” Smart materials and structures J, vol. 8, pp. 96-102, 1993.
- [30] H. Kwakernaak, “Robust control and  $H_{\infty}$  optimization,” Tutorial hper JFAC, Automatica, vol. 29, no. 2, pp. 255-273, 1993.
- [31] B. Miara, G. Stavroulakis, V. Valente, “Topics on mathematics for smart systems,” Proceedings of the European Conference. Rome, Italy, pp. 26-28, October 2006, World Scientific Publishers, Singapore, International, 2007.
- [32] M. Millston HIFOO 1.5: Structured control of linear systems with a non-trivial feedthrough. M.S. thesis, Courant Institute of Mathematical Sciences, New York University. 2006.
- [33] H. Kimura “Robust stability for a class of transfer functions”. IEE Transactions on Automatic Control, Vol. 29, pp. 788–793, 1984.
- [34] G. Zames, “Feedback minimax sensitivity and optimal robustness,” IEE Trans. Autom. Control, vol. 28, pp. 585–601, 1983.
- [35] W.S. Hwang, H. C. Park, “Finite element modeling of piezoelectric sensors and actuators”. AIAA journal J. Vol. 31, no. 5, pp. 930-937, 1993.
- [36] R. C. Ward, “Balancing the generalized eigenvalue problem”. SIAM J. Sci. Stat. Comput. Vol. 2, pp. 141-152, 1981.
- [37] G. Zames, “Feedback minimax sensitivity and optimal robustness”. IEE Transactions on Automatic Control. Vol. 28, pp. 585- 601, 1983.

**Citation:** Amalia Moutsopoulou, Georgios Stavroulakis, Tasos Pouliezios, “Robustness Issues in Intelligent Structures Using Nonconvex and Nonsmooth Optimization”, *International Journal of Emerging Engineering Research and Technology*, 8(2), 2020, pp. 9-16.

**Copyright:** © Amalia Moutsopoulou. This is an open-access article distributed under the terms of the Creative Commons Attribution License, which permits unrestricted use, distribution, and reproduction in any medium, provided the original author and source are credited.